International Journal of Engineering Works
Kambohwell Publisher Enterprises
ISSN: 2409-2770 Vol. 4, Issue 6, PP. 114-123, June 2017
www.kwpublisher.com

Surface Modification of Aluminum Alloy 6060 through Plasma Electrolytic Oxidation

Engr. Adnan Akbar, Muhammad Adnan Qaiser, Ahmad Hussain; Rajput Ali Mustafa, Prof. DanshengXiong

***Abstract*—**The impact of electrical parameters throughout PEO development so they can be upgraded to deliver coatings with improved properties were contemplated. Alumina coatings were generated on 6060 aluminum alloy substrates in a soluble silicate electrolyte utilizing a unipolar pulse DC current mode. The impact of preparing conditions, predominantly electrical parameters (frequency and duty cycle), on the arrangement, development conduct and properties of PEO coatings were researched. Distinctive portrayal techniques including scanning electron microscopy, energy dispersive X-ray spectroscopy, X-ray diffractometry, and contact tests were utilized to contemplate the microstructure, morphology and properties of the coatings. The connection between's the phase of the PEO procedure and the properties of the coating were appeared. The voltage-time reaction was observed to be critical since it gave promptly quantifiable and helpful data about these stages. It was found that the microstructure, morphology, development rate, stage conveyance and organization of coatings could be changed by shifting the electrical parameters.

***Keywords*—** Aluminium alloy, PEO, SEM, Friction coefficient, XRD, EDX.

I. INTRODUCTION

As of now, there is a push in the car business to additionally decrease vehicle weight. Worldwide patterns constrain the car business to make lighter, all the more earth friendly, more secure and more affordable autos [1].The main automakers are focusing on the lessening of auto weight and restricting the measure of fumes discharges because of administrative and shopper, necessities for more secure, cleaner vehicles [2]. As CO_2 outflow is in direct extent to fuel utilization auto weight has turned into the most basic measure of outline proficiency appraisals [3]. Weight lessening spare vitality as well as diminishes ozone harming substance outflows. Natural preservation is one of the essential explanations behind the emphasis of consideration on Al and its alloys. Environment preservation depends, as it were, on transportation industry, especially CO_2 outflows created by transport vehicles. European and North American auto makers have wanted to lessen fuel utilization by 25%, along these lines accomplishing a 30% CO_2 discharge diminishment by the year 2010 [4, 5].

A few surface change and coating arrangement have been created to upgrade the hardness, wear and corrosion resistance of Al alloys. These strategies have included thermal spraying [6], physical vapor deposition (PVD), chemical vapor deposition (CVD) [7, 9], ion implantation [10] and sol-gel coating [11]. Plasma Electrolyte Oxidation (PEO) is considered as the most financially savvy and earth cordial approach to enhance the corrosion and wear resistance of light components [12]. The PEO technique can be utilized to shape thick, hard, and exceptionally disciple clay like coatings on the surface of Al alloys and additionally the valve metals and their compounds. The oxide layers delivered on aluminum alloys can be subdivided in two-sub layers [13, 14]: a permeable external layer and a conservative interior layer. A few past reviews have researched the development instruments, and unrivalled tribological properties of PEO coatings created on various Al composite substrates [13, 16]. As a result, the surface properties gotten after PEO treatment are viewed as promising for modern application. PEO coatings have been produced for an extensive variety of modern applications including the material, gas and oil, car, gadgets, biomedical, aviation and metal framing enterprises [17, 19].

As of late, a few reviews have been led to better comprehend the way of the discharge technique and their impact on the systems of coating development [20, 21]. Plasma optical emission spectroscopy (OES) strategies have been utilized to portray PEO plasmas as far as electron fixation, ionization temperature, and component particular ion to atom arrangement [22, 23], and their associations with the layer development instruments. Such parameters are vital for better understanding and investigating electrolytic plasmas, a vital prerequisite for further improvement of PEO and related procedures [24]. In view of the OES comes about, and with a presumption of local thermodynamic equilibrium (LTE) [25], plasma electron temperatures have been computed utilizing the relative powers of ghastly lines of the same nuclear or ionic

Engr. Adnan Akbar: School of Material Science and Engineering, adnanakbarkhattak1983@gmail.com, Nanjing University of Science and Technology, Nanjing. Jiangsu, PR. China, +8613451825421.

Muhamad Adnan Qaiser: School of Material Science and Engineering, m.adnan.qaiser@gmail.com, Nanjing University of Science and Technology, Nanjing. Jiangsu, PR. China, +8613291263277

Ahmad Hussain: School of Material Science and Engineering, ahmed_00277@yahoo.com, Nanjing University of Science and Technology, Nanjing. Jiangsu, PR. China, +8615950472526

Rajput Ali Mustafa: School of Mechanical Engineering, mustafa11.amrr@gmail.com, Nanjing University of Science and Technology, Nanjing. Jiangsu, PR. China, +8618205084520

Prof. DanshengXiong: School of Material Science and Engineering, xiongds@163.com, Nanjing University of Science and Technology, Nanjing. Jiangsu, PR. China.

species [25]. The PEO innovation primarily frames an autogeneous oxide coating on the Al-compound surface and hypothetically does not expend the solute. Along these lines, the PEO innovation is a "spotless" treatment since it neither expends the cathode nor components in the electrolyte. The PEO procedure essentially shapes an Al_2O_3 coating which is metallurgically clung to the substrate and has high hardness, high impedance, and high soundness and gives Al-composite great seawater and high temperature consumption resistance.

II. EXPERIMENTAL WORK

In view of the different writings [5, 8, 15], numerous parameters influence the arrangement and microstructure of PEO coatings, as demonstrated in Figure. 1.

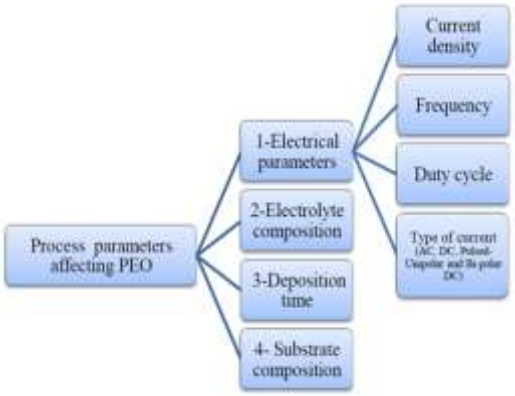

Figure. 1 Prepare parameters influencing the PEO coating process

A greatly extensive variety of electrolyte pieces has been utilized and there is a ton of information accessible. Electrical parameters additionally assume an essential part in the development of PEO coatings, despite the fact that the accessible writing is constrained. In this review all coatings were delivered on 6060 aluminum compound utilizing one substance recipe for the watery electrolyte. Every one of the coatings examined are delivered utilizing a unipolar beat DC control supply with a square waveform. The wave shape and comparing parameters of the unipolar beat control source are given in Figure. 2. Amid a solitary heartbeat, t_{on} and t_{off} are the periods amid which the current is on and off, individually. It is the beat on time (t_{on}) that assumes a significant part in the arrangement of the covering microstructure. Amid the beat off time (t_{off}), the miniaturized scale releases are hindered enabling the surface to cool.

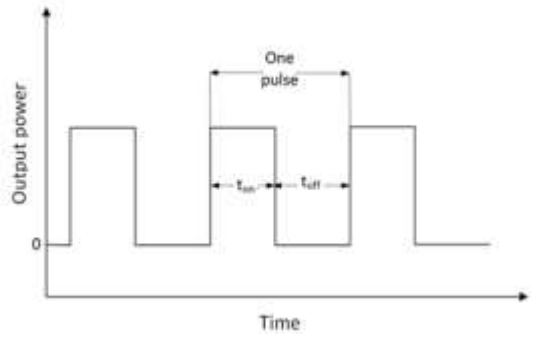

Figure. 2 Schematic of the beat unipolar yield of a PEO control source t_{on}: beat on time; t_{off}: beat off time

A PEO unit furnished with a DC control supply is utilized to deliver the coatings. The course of action of the gear utilized is shown in Figure. 3. The positive yield of the power supply is associated with the example drenched in the electrolyte as the working terminal (anode), and the negative yield is associated with the stainless steel electrolyte compartment, which gone about as the counter terminal (cathode). The specimen is rushed to a steel pole (protected by an artistic coat from the electrolyte) associated with the power supply. The specimens are covered under galvanostatic conditions, i.e. the current is kept steady amid the procedure and the anode potential is permitted to differ. To decide the required connected current to accomplish a particular current thickness (J) amid each heartbeat on time (t_{on}), the range of the specimen is measured and increased by the coveted current density.PEO coatings were readied utilizing diverse preparing conditions and distinctive portrayal strategies are utilized to concentrate the relationship between's covering parameters and qualities of the coatings including development microstructure and morphology, thickness, stage arrangement, mechanical properties and corrosion execution.

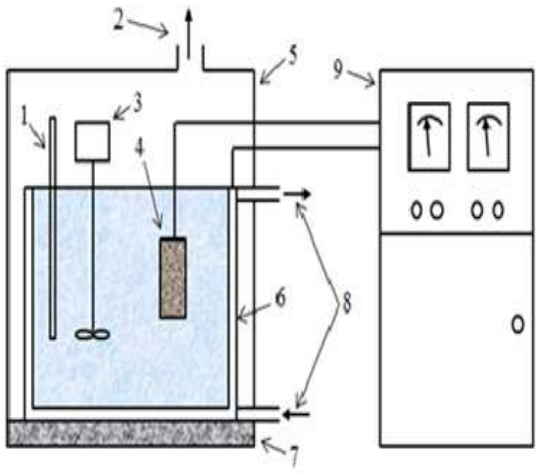

Figure. 3 Ordinary course of action of the gear utilized for PEO covering: (1) Thermocouple (2) Exhaust framework (3) Mixer (4) Work piece (5) Ground case (6) Bath (7) Insulating plate (8) Flow dissemination by means of cooling framework (9) Power supply unit

As said before PEO coatings were created utilizing the uni-polar beat DC mode with a square waveform connected at

ISSN: 2409-2770

various power frequencies of 400, 4000, 10000 and 20000 Hz. Two duty cycles (Dt), 80% and 20%, were utilized. At the recurrence of 10000 Hz two extra duty cycles of 10% and 50% were additionally utilized. The duty cycle is characterized as: $D_t = [t_{on}/(t_{on}+ t_{off})]\times100$ where t_{on} is the "on" length and t_{off} is the "off" span amid a solitary cycle. The PEO procedure was completed at a steady current density of 15 A/dm^2 for 10 minutes for all specimens. Tab.1 records the specimen codes and the preparing conditions.

The electrolyte was solution of 10 g/l Na_2SiO_3 and 2 g/l KOH in deionized water with a pH of 12.5. The electrolyte temperature was kept up in the scope of 33-38 °C amid treatment utilizing an outside warmth exchanger. Covering thickness was assessed utilizing an Eddy current gage.

TABLE. 1 PEO PREPARE PARAMETERS AND TEST CODES FOR COATING DEPOSITION ON 6060 AL ALLOY

Code	F (Hz)		D_t (%)	T_{on} (ms)	T_{off} (ms)
A1	f_1	400	20	500	2000
A2		400	80	2000	500
A3	f_2	4000	20	50	200
A4		4000	80	200	50
B1	f_3	10000	10	10	90
B2		10000	20	20	80
B3		10000	50	50	50
B4		10000	80	80	20
C1	f_4	20000	20	10	40
C2		20000	80	80	10

Twenty estimations were gone up against the covered surface of each specimen. Statistical techniques were connected to remove the mean information values and dissipate. Covering surfaces and cross areas were inspected utilizing examining electron magnifying instrument (SEM) furnished with a Quartz EDX framework. XRD was utilized to concentrate the stage synthesis of the coatings. The examples were checked in the 2θ territory from 20° to 80° with a 0.02 ° step estimate. So as to limit impedance from the substrate to the diffraction, glancing angle XRD was utilized with an edge of rate (α) set to 3.5°.

III. RESULTS AND DISCUSSION

Voltage-time reactions for PEO coatings framed utilizing the different duty cycles and frequencies are appeared in Figure. 4. As beforehand detailed [26-29], an underlying direct, unexpected voltage increment happens inside a brief timeframe taken after by a sudden lessening in incline of the voltage-time bend. The time when the slant of the voltage-time bend changes is assigned the starting, or breakdown, voltage. The PEO procedure is joined by starting miniaturized scale releases thus of dielectric breakdown [30-31], gas release [30], contact sparkle release [32] or any of their blends which is an exceptional component of PEO when contrasted with customary anodization [30].

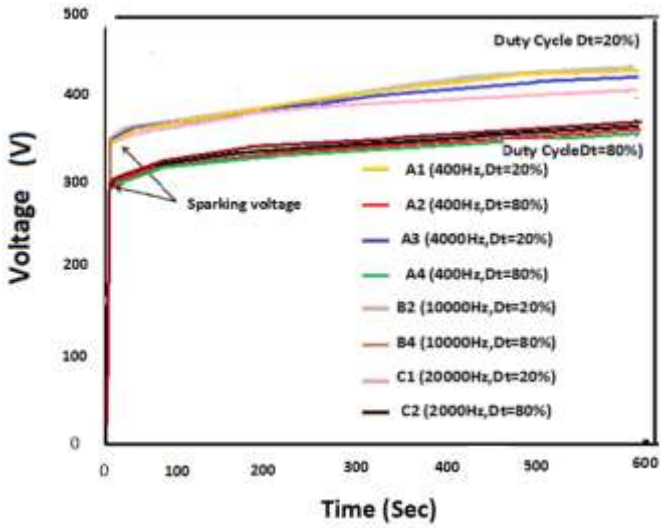

Figure. 4 Voltage-time reactions for PEO coatings at different duty cycles and frequencies

ISSN: 2409-2770

All through the PEO procedure the shading, power and thickness of miniaturized scale discharges always show signs of change. The shade of the small scale discharges changes from somewhat blue white to yellow and in the long run to orange while the power increments and thickness diminishes [33-35]. The starting or breakdown voltage and also the greatest voltage in the long run accomplished were higher in tests treated at duty cycle of 20% contrasted with those treated at duty cycle of 80%.

Figure. 5 exhibits the impact of duty cycle on the voltage-time reaction of coatings developed at a frequency of 10000 Hz. Diminishing the duty cycle from 80% to 10% was found tobring about higher breakdown and most extreme voltages. A correlation of the bends in Figure. 4 demonstrated no extensive contrast in starting and most extreme voltage come to amid PEO of tests treated at a similar duty cycle yet unique frequencies. Expanding the duty cycle result's in an expanded general power contribution to the framework. At higher duty cycles, the aggregate length of pulse beat on time in 10 min is more contrasted with lower duty cycles, and despite the fact that the voltages are for the most part higher at lower duty cycles, the result of the normal voltage and aggregate pulse on time term at a consistent current density is more prominent at higher duty cycles demonstrating a higher general power contribution to the framework.

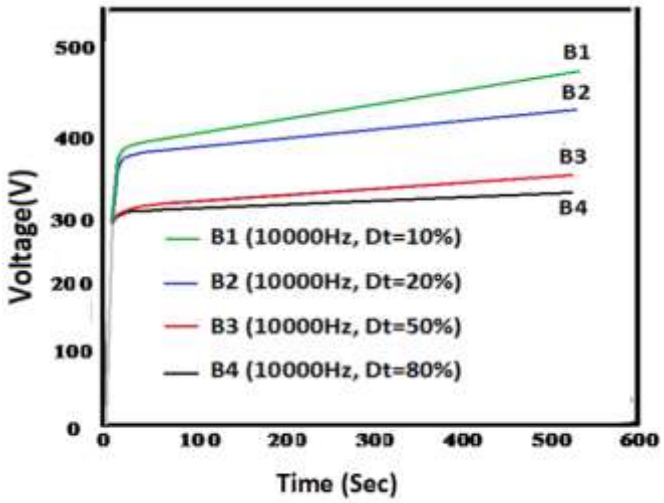

Figure. 5 Impact of duty cycle on the voltage-time reaction of coatings developed at a frequency of 10000 Hz

A normal SEM micrograph of a coated surface is appeared in Figure. 6. Two particular locales can be seen on the surface of all samples: a cratered structure with a focal gap (Area "b") and a lighter zone with a nodular structure (Area "a"). The focal gap in the cratered area is a release channel through which liquid material was shot out from the covering/substrate interface because of the high temperature and solid electric field. After launch this material quickly cemented upon contact with the electrolyte. EDX spectra measured at these two trademark locales are displayed in Figure. 7(a) and 7(b). The cratered district is rich in aluminum, reliable with its launch through the film from the substrate/covering interface. The nodular structure is rich in Si recommending it shaped by the co-affidavit of aluminum and silicon in the arrangement.

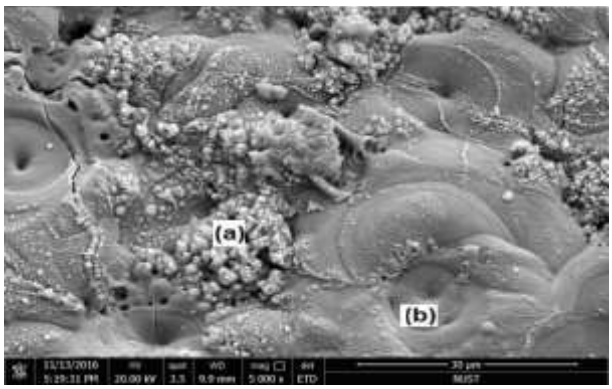

Figure. 6 SEM micrograph of a coated surface

It is for the most part accepted [33-37] that coating development is the consequence of the stream of oxidized liquid aluminum through release channels. The releases made amid PEO assume a key part in the coating development [42]. The size and surface components of the cavities could be an impression of the thickness and power of the releases [30, 38]; i.e., the more grounded the releases, the greater the pits. Figure. 8 shows the impact of the duty cycle on the span of pits. Picture investigation programming was utilized to gauge the extent of pits in the SEM micrographs and the deliberate

ISSN: 2409-2770

qualities were factually treated and announced. Since the power of the smaller scale releases shifts fundamentally amid the PEO procedure, the estimations of the cavity radii detailed here demonstrate a general pattern and ought not to be dealt with as quantitatively certain.

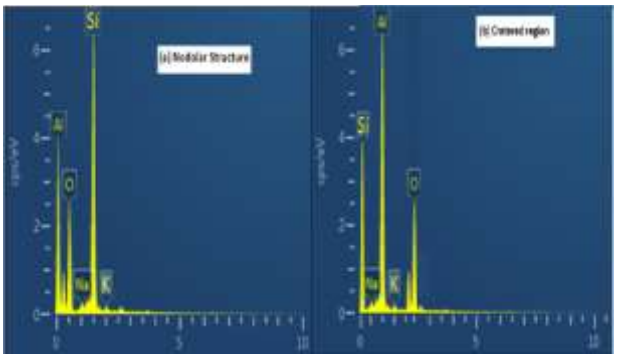

Figure. 7 (a) EDX spectra for nodular structure district (b) EDX spectra for cratered district

From Figure. 8 it is watched that the pit estimate tends to increment with expanding duty cycle, which could show upgraded or escalated small scale releases as the duty cycle increments. The impact of duty cycle on the surface morphologies of coatings shaped at a frequency of 10000 Hz is displayed in Figure. 9. Correlation of test B4 (Figure. 9(a), 80% duty cycle) with test B2 (Figure. 9(b), 20% duty cycle) demonstrates that less holes are framed on B4 and the surface is all the more thickly secured with nodular structures appeared to be rich in Si by EDX investigations.

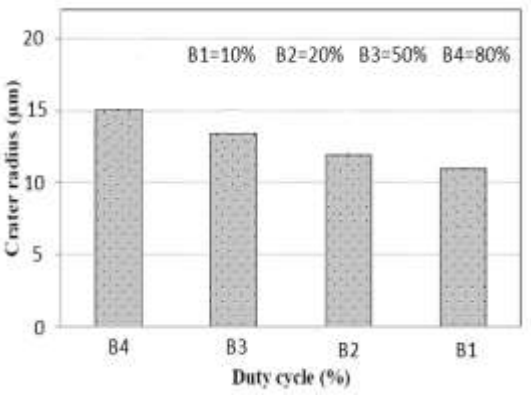

Figure. 8 Impact of the duty cycle on the magnitude of pits

The EDX elemental surface maps of tests C1 (20% duty cycle) and C2 (80% duty cycle) are looked at in Fig 10(a) and 10(b). The precision of the elemental concentration estimations may fluctuate in the vicinity of 2% and 7% [30]. It could be watched that a higher surface concentration of Al is acquired at a low, contrasted with a high, duty cycle. In actuality, the Si presence seems, by all accounts, to be higher at a higher duty cycle, however this is not as evident as on account of Al.

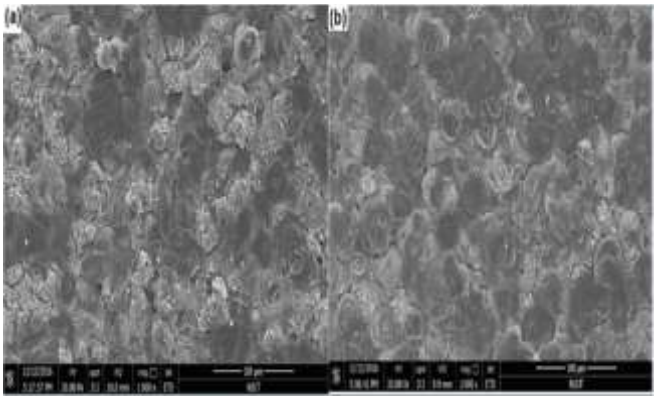

Figure. 9 (a) SEM micrographs of PEO coating surface of sample B4, D_t =80% from (Tab. 1)(b) SEM micrographs of PEO coating surface of sample B2, D_t =20% from (Tab. 1)

The Al/Si power proportions for various frequencies gotten from EDX basic surface mapping(Figure. 11) uncover that this proportion increments with diminishing duty cycle, reliable with the perceptions from Figure. 10. This recommends at a lower duty cycle more releases happened bringing about more Al taking part in the release procedure.

The outcomes exhibited in Figure. 4 to Figure. 11 affirm that the power of the miniaturized scale releases diminishes while their spatial thickness increments when a lower duty cycle is connected. As already specified that pits are the after effect of solid smaller scale releases brought about by dielectric breakdown of the coating that enter through its whole thickness. Accordingly, the bigger number of littler pits at low duty cycles (Figure. 7 and Figure. 8) proposes a higher number of flashes with lower power. One conceivable clarification for the lower force of miniaturized scale releases at low duty cycles could be the higher number of flashes at first glance. As the quantity of miniaturized scale releases expands, the current going through every individual small scale release-channel diminishes on the grounds that the general current is kept consistent, bringing about littler pit sizes (Figure. 8).

ISSN: 2409-2770

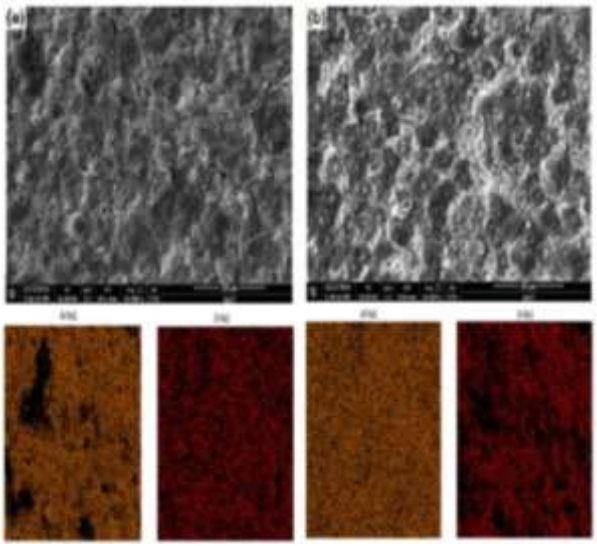

Figure. 10 (a) EDX basic diagram for test C2 80% duty cycle from (Tab. 1) (b) EDX basic diagram for tests C1 20% duty cycle from (Tab. 1)

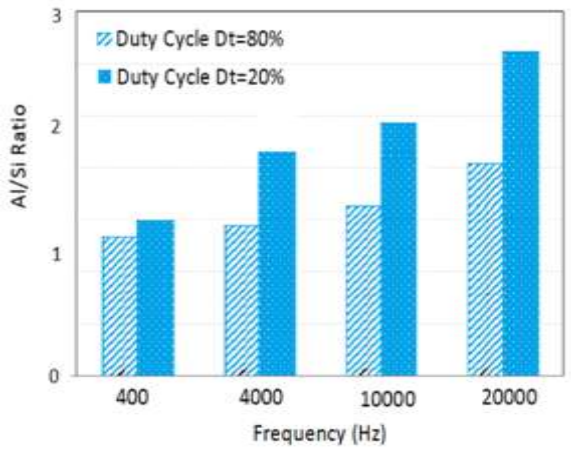

Figure. 11 Al/Si relative amount calculated from EDX basic diagrams

Thickness estimations (Figure. 12) demonstrate that the coating development rate increments step by step with diminishing duty cycle at consistent frequency. This expanded development rate at lower duty cycles could be connected to the way that coating development is the consequence of oxidized liquid aluminum as it streams out through release channels and more releases are included at lower duty cycles.

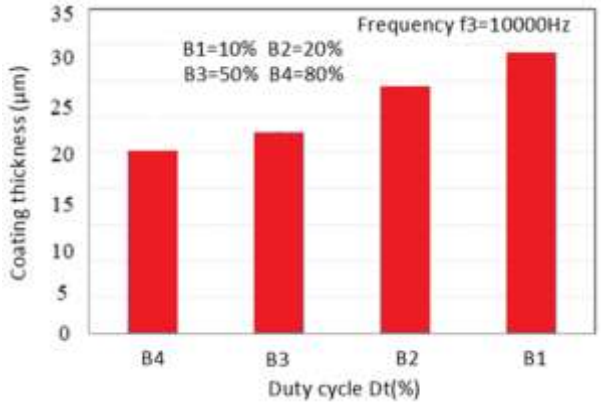

Figure. 12 Impact of duty cycle on coating development speed at frequency of 10000 Hz

The XRD tests of the coatings after PEO are shown in Figure. 12. The γ-Al_2O_3, α-Al_2O_3 and Al diffraction pinnacles were seen in the specimens. The outcomes recommend that the ceramic coating shaped contains predominantly α-Al_2O_3 and γ-Al_2O_3 stages. The presence of Al could be from the substrate impedance despite the fact that a moderately low angle (3.5°) of rate X-beam shaft was utilized. For instance in A3, B2 and C1 tests just γ-Al_2O_3 pinnacles were seen in the coatings; however in different examples, α-Al_2O_3 pinnacles were seen notwithstanding γ-Al2O3 crests. Alpha alumina is a steady, rhombohedral stage with a melting point of 2050 °C and gamma alumina is a cubic metastable stage that can change into α-Al_2O_3 if warmed in the scope of 800-1200 °C [27, 39, 40]. From the XRD comes about it can be found that for short ton times (B2 and C1 tests) the covering is for the most part made out of γ-Al_2O_3. As the ton time builds more γ to α alumina change happens and the measure of α alumina increments. At the point when the oxide is launched out of the channel, it quickly interacts with the electrolyte which brings about a high cooling rate.

ISSN: 2409-2770

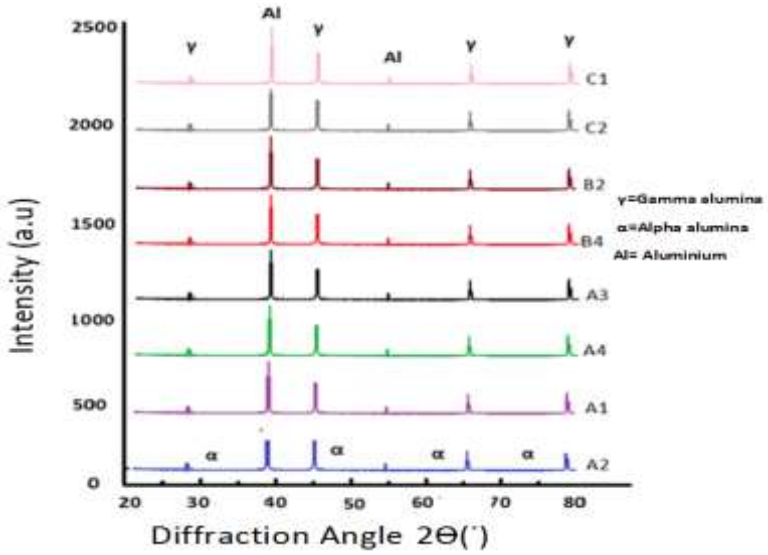

Figure. 13 XRD of coating tests from (Tab. 1)

It is recommended that homogeneous nucleation of the cementing of fluid beads at impressive under-cooling brings about the development of γ-Al_2O_3 as opposed to α-Al_2O_3 in light of its lower basic free vitality for nucleation. Be that as it may, because of the low warm conductivity of alumina covering, the temperature ascends in the covering as the procedure keeps, bringing on change of γ-Al_2O_3 to α - 3[33, 41]. Higher γ-Al_2O_3 stage content in tests with shorter ton times proposes that the temperature ascend in these specimens is lower and thus the $\gamma \rightarrow \alpha$ -Al_2O_3 change which requires warmth is hindered.

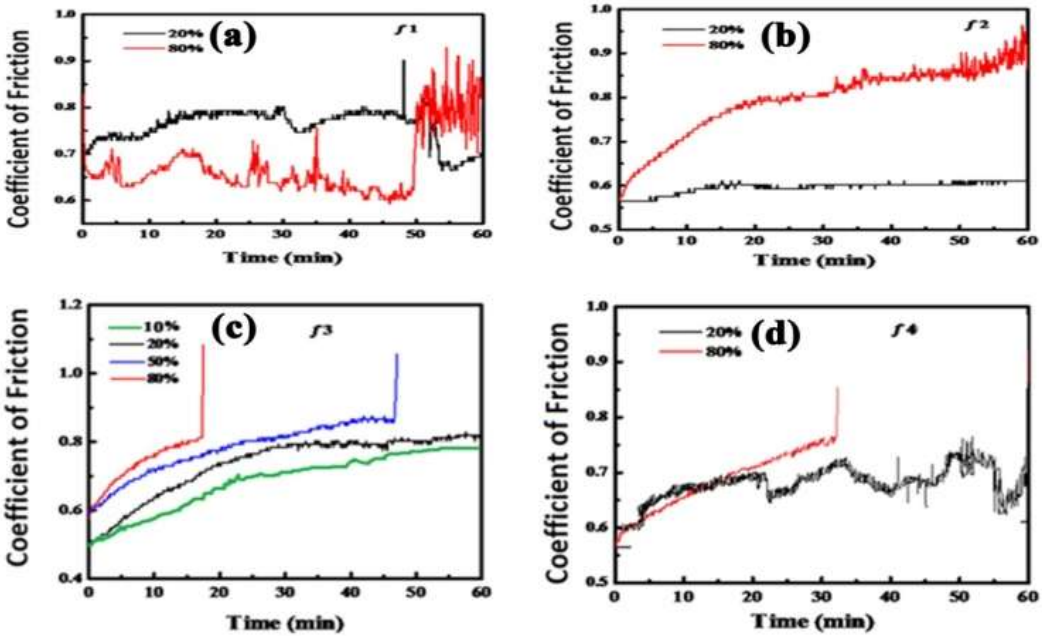

Figure. 14(a) Coefficient of friction verses time response for specimen A1 and A2 at frequency 400 Hz (b) Coefficient of friction verses time response for specimen A3 and A4 at frequency 4000 Hz (c) Coefficient of friction verses time response for specimen B1, B2, B3 and B4 at frequency 10000 Hz (d) Coefficient of friction verses time response for specimen C1 and C2 at frequency 20000 Hz

ISSN: 2409-2770

Figure. 14(a-d) demonstrate the coefficient of friction Vs time reaction for Al tests coated at frequencies 400 Hz, 4000 Hz, 10000 Hz and 20000 Hz. It is so clear from Figure. 14(a) to (d) that the friction coefficient is high for low duty cycles at lower frequency. Be that as it may, when the frequency is expanded the coefficient of friction is diminished for low duty cycles. In this manner tests PEO coated at high duty cycle and high frequency has more coefficient of friction as analyzed specimens PEO coated at low duty cycle and low frequency.

The reason behind this behavior could be because of the presence of high γ-phase and low α-phase alumina on the surface of the coated aluminium alloy at high frequency and high duty cycle resulting in high coefficient of friction and vice versa. Therefore at high frequency and high duty cycle friction rate is high as compared at low frequency and low duty cycle.

During pin on disc friction test experiment on PEO coating samples different disc radii 3R, 5R and 7R were used to see any change in the friction coefficient by changing the disc radius. From Figure. 15 (a-d) it is noted that there is no such effect on the coefficient of friction by changing the disc radius which suggests that the surface coated by PEO process is more homogenous.

CONCLUSION

The PEO preparing of the 6060 aluminum composite utilizing distinctive frequencies and duty cycles was researched. It was found that the microstructure, morphology, development rate, stage dispersion and creation of coatings could be changed by fluctuating the electrical parameters. At low duty cycles the starting and most extreme voltages were both higher.

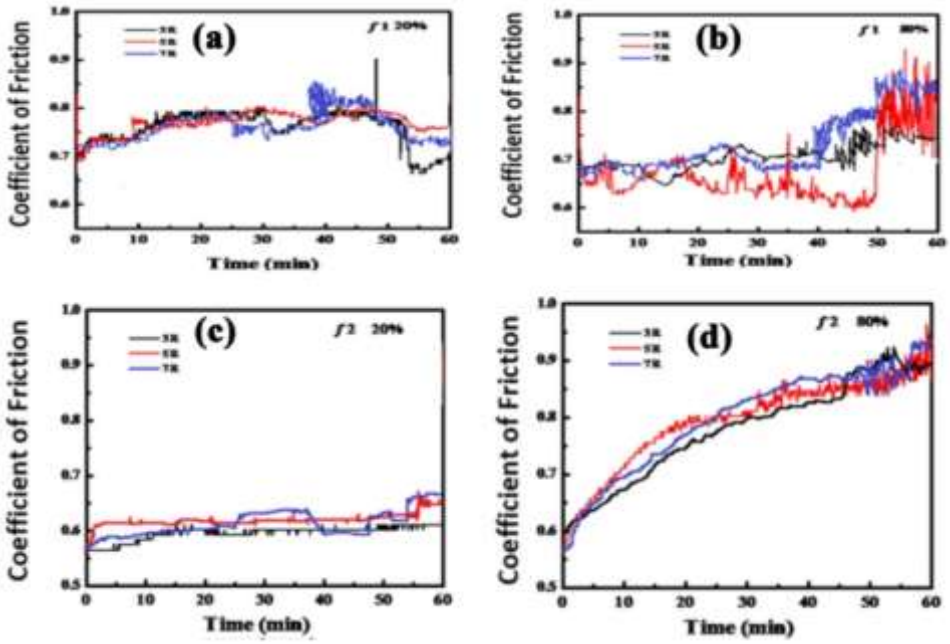

Figure. 15 (a) Coefficient of friction verses time response for test specimen A1 at disc radius 3R, 5R, 7R (b) Coefficient of friction verses time response for test specimen A2 at disc radius 3R, 5R, 7R (c) Coefficient of friction verses time response for test specimen A3 at disc radiius 3R, 5R, 7R (d) Coefficient of friction verses time response for test specimen A4 at disc radius 3R, 5R, 7R

Two areas were seen on the surface of all examples: (a) cratered locales, rich in aluminum, with release directs in the inside, inferring they were the aftereffect of dielectric breakdown over the coating, and (b) a nodular structure, rich in silicon. Applying lower duty cycles created miniaturized scale releases with higher spatial thickness and lower power. These gentler miniaturized scale releases made littler pits. Amid the PEO procedure at high duty cycles, smaller scale releases ended up plainly more grounded however their number diminished, particularly at longer circumstances. Nonetheless, at lower duty cycles the surface of the specimen was completely secured by flashes notwithstanding amid the last stages.

The sparking conduct brought on by the use of various electrical parameters influenced the silicon circulation. Low duty cycles brought about a lower centralization of Si on the surface and its more uniform conveyance over the coating. This marvel could be attributed to the higher thickness of sparkles at low duty cycles which separates adsorbed silicon containing species from the surface of the specimen and furthermore more grounded electric fields which increment the likelihood of joining of Si rich anions into the coating. XRD designs uncovered that electrical parameters influence the $\gamma \rightarrow \alpha$ -

ISSN: 2409-2770

Al_2O_3 stage change. For A3, B2 and C1 tests in which ton times were short, 50, 20 and 10 milliseconds individually, just γ -Al_2O_3 pinnacles were watched. However, for different examples with longer ton times, α-and γ-Al_2O_3 coincide. From Friction test examination it is watched that at lower duty cycle and low frequency the friction coefficient is high and the other way around. It is normal the outcomes introduced here could be used to better control the PEO procedure so as to deliver coatings with fancied properties.

REFERENCES

[1] C. Blawert, N. Hort and K. Kainer. "Automotive applications of magnesium and its alloys," Trans Indian Inst Met,2004, 57(4): 397-108.

[2] H. Friedrich and S. Schumann. "Research for a new age of magnesium in the automotive industry," Journal of Materials Processing Technology,2001 117: 276-281.

[3] J.J. Michalek, P.Y. Papalambros and S.J. Skerlos. "A study of fuel efficiency and emission policy impact on optimal vehicle design decisions," J Mech Des, 2004, 126(6): 1062-1070.

[4] H. Dieringa and K.U. Kainer. "Magnesium der Zukunftswerkstoff fur die Automobilindustrie," Material wissenschaft und Werkstofftechnik, 2007, 38(2): 91-95.

[5] E. Aghion, B. Bronfin, D. Eliezer. "The role of the magnesium industry in protecting the environment," Journal of Materials Processing Technology,2001, 117(3): 381-385.

[6] Y. Sun. "Thermally oxidised titanium coating on aluminium alloy for enhanced corrosion resistance," Materials Letters,2004, 58: 2635-2639.

[7] X. Zhang, S. Lo Russo, S. Zandolin, A. Miotello, E. Cattaruzza and P.L. Bonora. "The pitting behavior of Al-3103 implanted with molybdenum," Corrosion Science,2001, 43: 85-97.

[8] P. Preston, R. Smith, A. Buchanan and J. Williams. "Characterization of blister formation and pitting of tungsten ion implanted aluminium," Scripta Metallurgica et Materialia,1995, 32: 2015-2020.

[9] M. Sheffer, A. Groysman and D. Mandler. "Electro deposition of sol-gel films on Al for corrosion protection," Corrosion Science,2003, 45: 2893-2904.

[10] J. Masalski, J. Gluszek, J. Zabrzeski, K. Nitsch and P. Gluszek. "Improvement in corrosion resistance of the 3161 stainless steel by means of AI2O3 coatings deposited by the sol-gel method," Thin Solid films,1999, 349(1-2): 186-190.

[11] J. Zhao, J. Xia, A. Sehgal, D. Lu, R. McCreery and G. Frankel. "Effects of chromate and chromate conversion coatings on corrosion of aluminum alloy 2024- T3," Surface and Coatings Technology,2001, 140: 51-57.

[12] A. L. Yerokhin, X. Nie, A. Leyland, A. Matthews and S. J. Dowey. "Plasma electrolysis for surface engineering," Surface and Coatings Technology,1999, 122: 73-93.

[13] L. O. Snizhko, A. L. Yerokhin, A. Pilkington, N. L. Gurevina, D. O. Misnyankina, A. Leyland and A. Matthews. "Anodic processes in plasma electrolytic oxidation of aluminum in alkaline solutions," Electrochimica Acta,2004, 49: 2085-2095.

[14] W. Xue, Z. Deng, R. Chen and T. Zhang. "Growth regularity of ceramic coatings formed by micro arc oxidation on Al[Cu]Mg alloy," Thin Solid Films,2000, 372: 114-117.

[15] F. Mecuson, T. Czerwiec, T. Belmonte, L. Dujardin, A. Viola and G. Henrion ,"Diagnostics of an electrolytic microarc process for aluminum alloy oxidation," Surface and Coatings Technology,2005, 200: 804-808.

[16] A.V. Timoshenko and Y.V. Magurova. "Investigation of plasma electrolytic oxidation processes of magnesium alloy MA2-1 under pulse polarization modes," Surface and Coatings Technology,2005, 199: 135-140.

[17] H. Ryu, S. Hong. "Corrosion Resistance and Antibacterial Properties of Agcontaining MAO coatings on AZ31 Magnesium Alloy Formed by Microarc Oxidation," Journal of Electrochemical Society,2010, 157 (4): C131-C136.

[18] X. Nie, X. Li, D. Northwood. "Corrosion behavior of metallic materials in ethanolgasoline alternative fuel cell," Materials Science Forum,2007, 546-549: 1093-1100.

[19] P. Zhang, X. Nie, D. Northwood. "Influence of coating thickness on the galvanic corrosion properties of Mg oxide in an engine coolant," Surface and Coatings Technology,2009, 203: 3271-3277.

[20] C. S. Dunleavy, I. O. Golosnoy, J. A. Curran and T. W. Clyne. "Characterization of discharge events during plasma electrolytic oxidation," Surface and Coatings Technology,2009, 203: 3410-3419.

[21] A. L. Yerokhin, L. O. Snizhko, N. L. Gurevina, A. Leyland, A. Pilkington and A. Matthews. "Discharge characterization in plasma electrolytic oxidation of aluminium,"J. Phys. D: Appl. Phys.,2003, 36: 2110-2120.

[22] M. D. Klapkiv, H. M. Nykyforchyn and V. M. Posuvailo. "Spectral analysis of an electrolytic plasma in the process of synthesis of aluminum oxide," Mat. Sci.,1995, 3: 333-343.

[23] F. Me'cuson, T. Czerwiec, G. Henrion, T. Belmonte, L. Dujardina, A. Viola, J Beauvir. "Tailored aluminum oxide layers by bipolar current adjustment in the Plasma Electrolytic Oxidation (PEO) process," Surface and Coatings Technology,2007, 201: 8677-8682.

[24] A. I. Maximov and A. V. Khlustova. "Optical emission from plasma discharge in electrochemical systems applied for modification of material surfaces," Surface and Coatings Technology,2007, 201: 8782-8788.

[25] H. R. Griem, Plasma Spectroscopy, Cambridge: McGraw-Hill, 1964.

[26] F. Monfort, A. Berkani, E. Matykina, P. Skeldon, G.E. Thompson, H. Habazaki, et al. "Development of anodic coatings on aluminium under sparking conditions in silicate electrolyte," Corros. Sci., 2007, 49: 672–693.

[27] G. Lv, W. Gu, H. Chen, W. Feng, M.L. Khosa, L. Li, et al. "Characteristic of ceramic coatings on aluminum by plasma electrolytic oxidation in silicate and phosphate electrolyte," Appl. Surf. Sci, 2006, 253: 2947–2952.

[28] K.M. Lee, Y.G. Ko, D.H. Shin. "Incorporation of multi-walled carbon nanotubes into the oxide layer on a 7075 Al alloy coated by plasma electrolytic oxidation: Coating structure and corrosion properties," Curr. Appl. Phys., 2011, 11: S55–S59.

[29] F. Monfort, E. Matykina, A. Berkani, P. Skeldon, G.E. Thompson, H. Habazaki, et al. "Species separation during coating growth on aluminium by spark anodizing," Surf. Coatings Technology, 2007, 201: 8671–8676.

[30] R.O. Hussein, X. Nie, D.O. Northwood, A. Yerokhin, A. Matthews. "Spectroscopic study of electrolytic plasma and discharging behavior during the plasma electrolytic oxidation (PEO) process," J. Phys. D. Appl. Phys., 2010, 43: 105203–105216.

[31] H. Wu, J. Wang, B.B. Long, Z. Jin, W. Naidan, F. Yu, et al. "Ultra-hard ceramic coatings fabricated through microarc oxidation on aluminium alloy," Appl. Surf. Sci., 2005, 252: 1545–1552.

[32] A.L. Yerokhin, L.O. Snizhko, N.L. Gurevina, A. Leyland, A. Pilkington, A. Matthews. "Discharge characterization in plasma electrolytic oxidation of aluminium," J. Phys. D. Appl. Phys., 2003, 36: 2110–2120.

[33] G. Sundararajan, L. Rama Krishna. "Mechanisms underlying the formation of thick alumina coatings through the MAO coating technology," Surf. Coatings Technol., 2003, 167: 269–277.

[34] J.M. Wheeler, J. A. Curran, S. Shrestha. "Microstructure and multi-scale mechanical behavior of hard anodized and plasma electrolytic oxidation (PEO) coatings on aluminum alloy 5052," Surf. Coatings Technol., 2012, 207: 480–488.

[35] A.L. Yerokhin, X. Nie, A. Leyland, A. Matthews, S.J. Dowey. "Plasma electrolysis for surface engineering," Surf. Coatings Technol., 1999, 122: 73–93.

[36] F. Jaspard-mécuson, T. Czerwiec, G. Henrion, T. Belmonte, L. Dujardin, A. Viola, et al. "Tailored aluminium oxide layers by bipolar current adjustment in the Plasma Electrolytic Oxidation (PEO) process," Surf. Coatings Technol., 2007, 201: 8677–8682.

[37] L. Rama Krishna, K.R.C. Somaraju, G. Sundararajan. "The tribological performance of ultra-hard ceramic composite coatings obtained through microarc oxidation," Surf. Coat. Technol., 2003, 163: 484–490.

[38] R.O. Hussein, D.O. Northwood, X. Nie. "Coating growth behavior during the plasma electrolytic oxidation process", J. Vac. Sci. Technol. A Vacuum," Surfaces Film, 2010, 28: 766–773.

[39] R.H.U. Khan, A. Yerokhin, X. Li, H. Dong, A. Matthews. "Surface characterization of DC plasma electrolytic oxidation treated 6082 aluminium alloy: Effect of current density and electrolyte concentration," Surf. Coatings Technol., 2010, 205: 1679–1688.

[40] C.J.-P. Steiner, D.P.H. Hasselman, R.M. Spriggs. "Kinetics of the Gamma-to-Alpha Alumina Phase Transformation," J. Am. Ceram. Soc., 1971, 54: 412–413.

[41] R. McPherson. "Formation of metastable phases in flame- and plasma-prepared alumina," J. Mater. Sci., 1973, 8: 851–858.

[42] C.S. Dunleavy, I.O. Golosnoy, J. A. Curran, T.W. Clyne. "Characterization of discharge events during plasma electrolytic oxidation," Surf. Coatings Technol., 2009, 203: 3410–34.